MECHANICAL PROPERTIES AND MICROSTRUCTURES OF ADDITIVELY MANUFACTURED 950 PLATINUM RUTHENIUM ALLOY

Teresa Frye

Given that additively manufactured (AM) platinum alloys are relatively new to the market, early adopters benefit from increasing data on their material properties. The alloy 95% platinum 5% ruthenium (950 PtRu) is widely used across the United States in cast and fabricated forms, however there is scant data in the literature for AM outputs of this alloy. The present work reports mechanical properties and microstructures for Direct Metal Laser Sintered (DMLS) 950 PtRu in the as-printed and hot isostatic pressed conditions and further offers comparisons with investment cast samples produced in the same alloy to highlight differences in material properties for each method of manufacture.

Teresa Frye is the Founder of TechForm Advanced Casting Technology in Portland, Oregon. TechForm provides platinum castings to a broad customer base, including many of the top jewelry brands in the US. In the early 90s her firm introduced high-temperature casting methods from the aerospace industry to platinum manufacturing. A leading expert on shell casting methods and a prolific researcher, she has published numerous technical papers and articles worldwide. Her publications have appeared in the Johnson Matthey Technology Review, The Santa Fe Symposium® on Jewelry Manufacturing Technology, The Metal Powder Industries Federation, The Jewelry Technology Forum, MJSA Journal, and JCK Magazine, among others. She has also presented her research at numerous venues across the globe.

MECHANICAL PROPERTIES AND MICROSTRUCTURES OF ADDITIVELY MANUFACTURED 950 PLATINUM RUTHENIUM ALLOY

Teresa Frye
Founder

Joel Meltzer, Kevin Mueller

TechForm Advanced Casting Technology, LLC
Portland, OR, USA

Mark Lisin
Lisin Metallurgical Services, LLC
Portland, OR, USA

INTRODUCTION

Platinum alloys are the material of choice for many industries due to their resistance to chemical corrosion, good wear resistance, biocompatibility, and suitable mechanical properties at highly elevated temperatures. The Additive Manufacturing (AM) process Laser Powder Bed Fusion (LPBF) is a process of selectively laser melting of individual particles of metal to create a 3D object. LPBF offers several advantages over conventional casting and machining processes for platinum alloys including the ability to create highly complex geometries with superior mechanical properties in as little as just a few hours. Prior research for AM Pt alloys suggests several notable trends in mechanical properties and microstructures when compared to their cast counterparts; grain size and morphology as well as strength and hardness have been demonstrated as unique and generally more favorable for 950 Pt components produced through AM.[1,4] One of the most compelling traits is the relatively fine grain structure AM methods yield in comparison to investment cast products, suggesting the presence of a Hall-Petch relationship.

For example, Laag and Heinrich[1] report grain size in a LPBF 950 PtAuIn alloy as small as 20 µm, which they note is essentially impossible to produce in cast products. Earlier research by Zito[3] confirmed grain size of approximately 30 µm in a 950 Pt alloy that was attributed to the rapid cooling of molten metal inherent in AM build processes that utilize laser melting.

Notwithstanding superior mechanical properties and microstructures, at the time of this writing barriers to large scale adoption of AM platinum alloys do exist, including a scarcity of powder vendors and the relatively high cost of producing powder compared to traditional platinum alloy melt stocks such as casting grain. Surface finishes from LPBF are also known to be rougher than typical cast or machined products, a feature of particular concern in the jewelry industry where high-polished areas with small cross sections are frequently used.

The present work aims to gain a deeper understanding of the mechanical properties and microstructures of LPBF 950 PtRu in the as-printed and hot isostatic pressed (HIP) conditions. Results are further compared with mechanical properties and microstructures of investment cast 950 PtRu in the as-cast and HIP conditions to determine whether opportunities for improved performance exist for one method over the other.

1. MATERIALS & METHODS

1.1 Sample Sources

Two different facilities provided LPBF samples for this study in order that we could obtain a broader sampling of operators. The facilities and alloys are as follows:

Facility A: LPBF of 95% Pt 5% Ru with machine as described in section 2.3 (A is our in-house facility).

Facility B: LPBF of 95% Pt 5% Ru with machine as described in section 2.3 (B is vendor facility)

1.2 Alloy Powder

Gas atomized powder composed of 95% Platinum 5% Ruthenium (950 PtRu) was selected for LPBF components at both facilities sampled in this study. PtRu was chosen to its prevalence in the US market for jewelry and the available powder compatible with the LPBF systems used. Comprehensive data on properties for investment cast 950 PtRu is also well-established,[7] a key benefit towards comparing AM product output versus current mainstream methods of manufacture. The 950 PtRu powder used in the trials ranged in particle size from 15 to 54 µm. For this batch, the D10 is 12.58 D50 is 21.5m and the D90 is 44.8microns, as measured by laser diffraction. Because recycling of Pt alloy powder is a standard method in LPBF processes, this was also done in the present trials. All powder was screened through a 63 µm sieve before each run using recycled powder.

1.3 LPBF Machine

An EOS Precious M80 machine was used at both facilities to produce the samples. The machine has a nominal laser power of 100 watts and an expected power in the building area of 85 watts. The laser type is Ytterbium fiber with a wavelength of 900-1200 nm and a spot size of 22 micron. The parameters used are confidential and therefore not cited in this work.

1.4 Platinum Casting

A centrifugal induction casting machine with optical pyrometer for temperature control was used for the casting experiments. Casting parameters for the 950 PtRu[2] samples are shown in Table 1.

Table 1: Casting parameters for Facility A 950 PtRu test bars and ring samples

Pour Temp ° C/°F	Flask Temp ° C/°F	RPM	Atmosphere
1873/3398	850/1562	400/1	Argon Only

1.5 Hot Isostatic Pressing

HIP was performed using proprietary parameters specifically developed for 950 platinum alloys and routinely used on cast 950 PtRu. HIP is a well-known densification process that uses heat and pressure as an effective means of removing internal porosity in castings and has been more recently adopted for AM components. Mechanical properties, particularly those that measure ductility such as elongation and reduction of area, will typically improve significantly through use of the HIP process.[8]

1.6 Mechanical Testing

Tensile testing was done in accordance with ISO 6892-1. A quantity of eight test bars (4 as-printed; 4 HIP; without machining) was produced with the geometry and build orientation shown in Figure 1. A horizontal (XY) orientation was used due to high platinum alloy costs of building eight bars in the vertical (Z) direction. In addition, a previous study reported more favorable UTS in the horizontal versus vertical orientation in an 80Pt20Ir alloy due to anisotropic behavior.[1] Although we did not know if this would be the case for our specific alloy and build parameters, we opted for a horizontal build as the most economical approach.

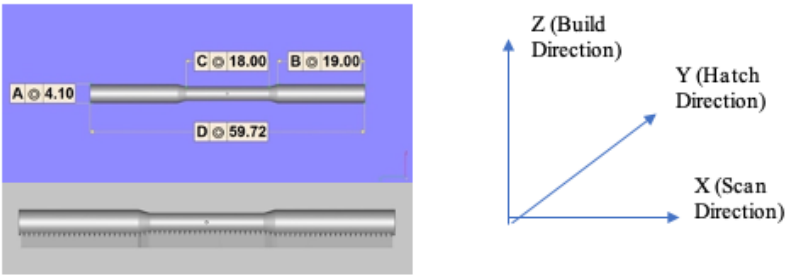

Figure 1: Tensile bar (units in mm) with supports for horizontal build orientation

Microhardness testing for all samples (LPBF and investment cast) was done in accordance with ASTM E 384 with a load of 1 kg. Five indents per sample were taken and averaged for the reported results.

1.7 Samples and Preparation

Figure 2 (left) shows the simple ring geometry that was used to assess porosity levels and qualitative grain size for the LPBF samples produced at Facility A, as well as the investment cast samples. Facility B used a wedding band as shown in Figure 2 (right). All rings were sectioned transverse to the axis as indicated by the red line in Figure 2, followed by mounting in epoxy and polishing/etching as follows:

- Strip grinding on 240 grit to remove saw cuts and establish flat plane
- Strip grinding on 320, 400, and 600 grit successively with light pressure and rotation of the metallographic mount on each pass
- 6-micron diamond polish with little pressure
- 1-micron alumina polish with little pressure
- Brief ultrasonic cleaning performed after each step to avoid contamination
- Electrolytic etch using HCL NaCl mixture and 4V AC for 2-4 minutes

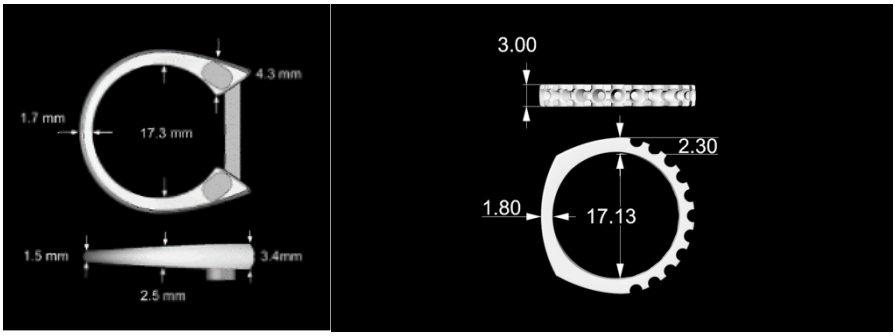

Figure 2: Ring geometries (in mm) for porosity assessment with sectioning transverse to the axis

1.8 Optical Microscopy

An optical metallograph was used to image the metallographic sections. Brightfield illumination was used in all cases. Metallographic sections were examined in the as-polished and etched conditions. Porosity was quantified using Pax-it image analysis software.

1.9 Scanning Electron Microscopy (SEM)

SEM was used to image fracture surfaces and metallographic sections using secondary and backscattered electron detectors. All images were acquired at an accelerating voltage of 20 kV.

1.10 Surface Finish Measurements

Surface finish was characterized per ISO 4287 using a 0.8 mm Gaussian filter and a non-contact optical profilometer. The arithmetic average (Ra) of five 2 mm long linear scans was measured in each of the radial and circumferential directions.

2. RESULTS

2.1 Powder Characterization

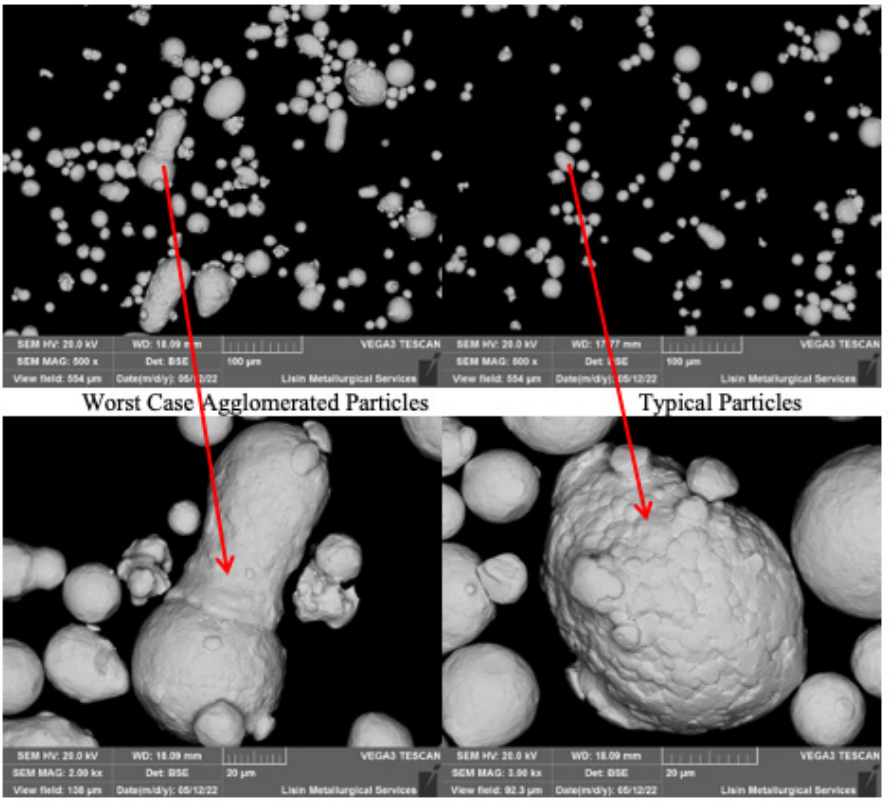

Figure 3: SEM analysis of 950 PtRu (post-print) recycled powder

Figure 3 contains backscattered electron images acquired from the recycled 950 PtRu powder sample after sieving with a 63 µm calibrated sieve. The majority of the sample (represented by the image at upper right) consisted of fine, spherical, 10 to 50 µm diameter particles consistent with the originally specified 15 to 54 µm particle size range. Larger, 50 to 100 µm particles appeared to consist of fused agglomerations of finer particles. The coarser agglomerated particles may represent debris generated by partial fusion of detached particles formed during processing. The question of effective sieving arises when we consider a 100 µm particle in our sieved material. As shown in Figure 3, many of these particles are elongated and have widths that are at or less than the 63 µm sieve opening.

2.2 Mechanical Properties

Results from mechanical properties testing of LPBF test bars produced at Facility A are compared to investment casting properties shown in Table 2 and Figure 4. Tensile values are an average of four tests, while hardness values are an average of five measurements.

Table 2: Mechanical properties comparison Facility A 950 PtRu LPBF vs. investment cast 950 PtRu

Variant		UTS (MPa)	Yield (MPa)	Elongation %	ROA%	HV 1
950 PtRu LPBF (XY) As-Printed Facility A	Average	537	444	29.3	61.9	163
950 PtRu LPBF (XY) +HIP Facility A	Average	499	350	41.5	83.5	156
950 PtRu As-Cast Facility A	Average	411	229	30	61	129
950 PtRu Cast + HIP Facility A	Average	419	235	38	89	125

Consistent with previous data reported in the literature,[1,4] strength and hardness are notably higher for the AM method of manufacture versus investment casting. A 93% increase in yield strength (YS) MPa value and a 30% increase in ultimate tensile strength (UTS) MPa value is seen in the as-printed compared to as-cast test bars; for HIP samples an increase of 49% and 19% respectively was observed. Hardness also shows an increase for the LPBF sample in the range of 25% for both as-printed / as-cast and HIP conditions. Of note is the significant drop in values for UTS and especially Yield for LPBF test bars in the HIP condition. Given that grain growth was not observed (Figure 13) this is likely a result of annealing during HIP. Specifically, steep thermal gradients during deposition likely lead to high residual stresses and a high dislocation density not unlike a cold worked structure. HIP can relieve these residual stresses and in so doing soften the material. Ductility values, on the other hand, are nearly the same for both LPBF and Casting; Elongation and ROA both show improved values due to the elimination of sub-surface porosity in the HIP condition. Extensive necking shown in the spent LPBF tensile bars with and without HIP (Figure 5) demonstrates a very ductile material. The fracture is an oval shape with the major axis parallel to the build direction. The oval fracture is a clear indication of anisotropy, as also reported for LPBF test bars by Laag and Heinrich.[1]

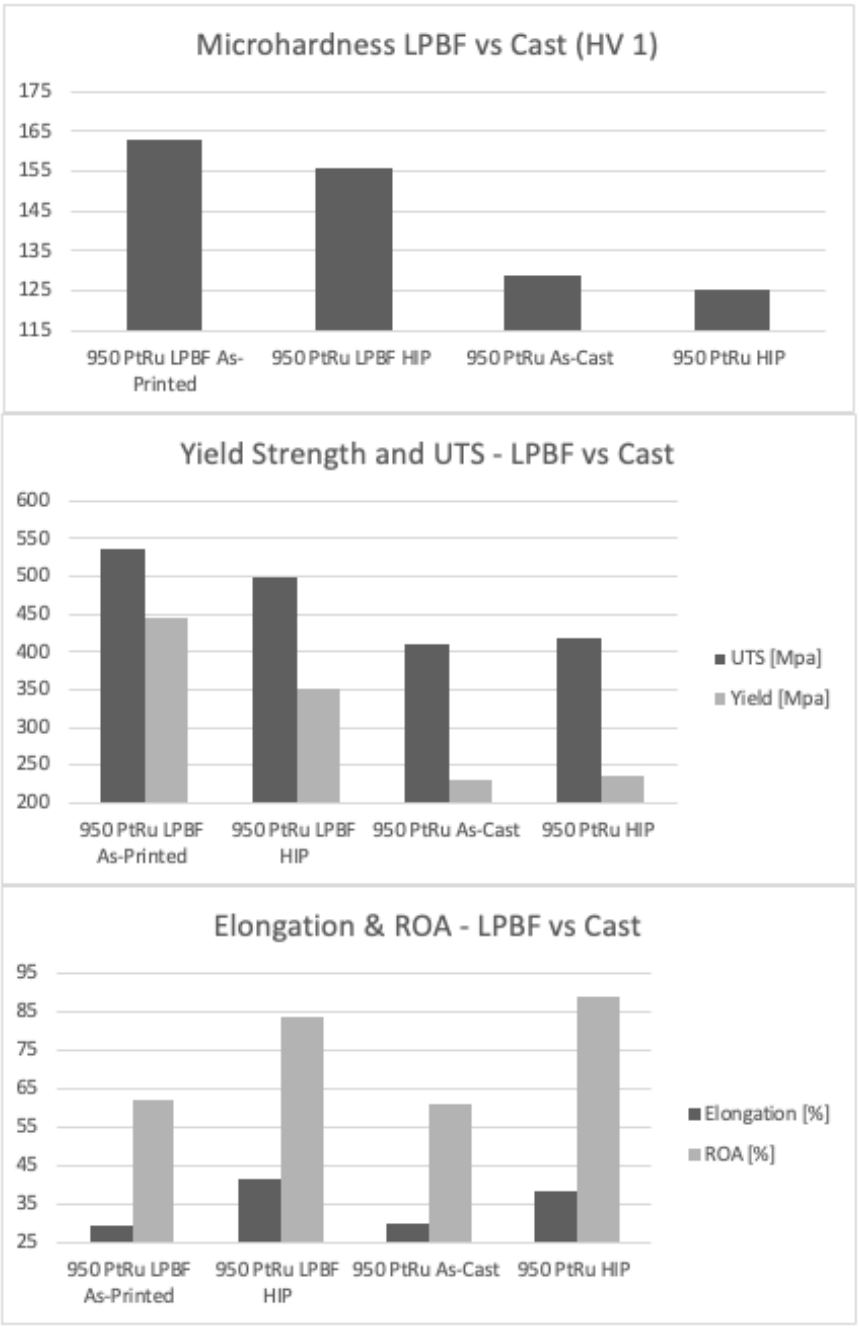

Figure 4: Tensile and hardness properties LPBF as-printed and HIP; castings as-cast and HIP

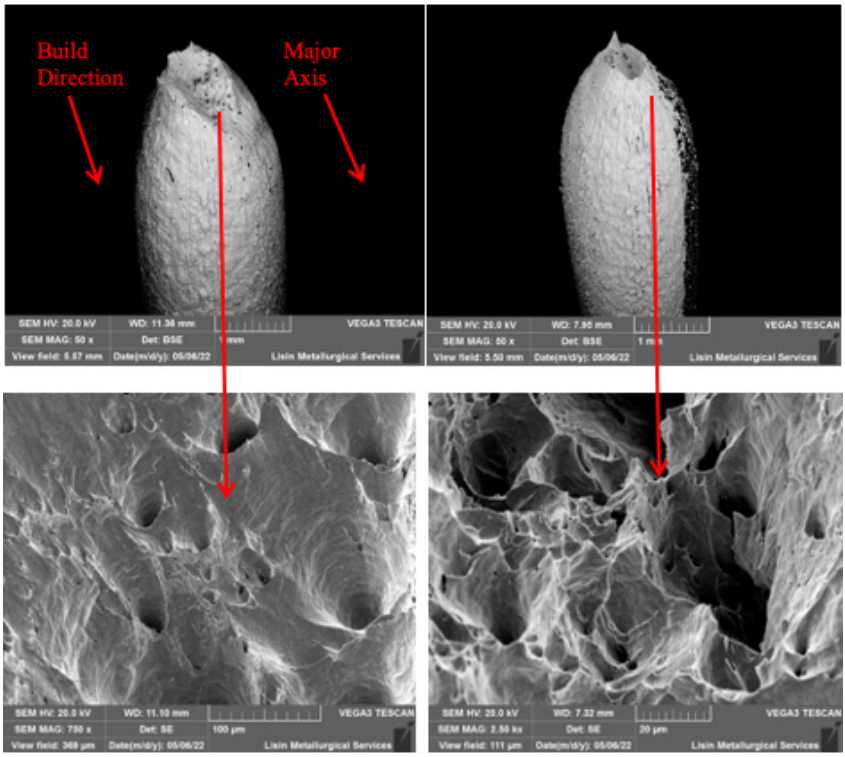

Figure 5: Spent LPBF 950 PtRu tensile bars as-printed (left) and HIP (right) display ductile fractures

2.3 Microstructure Evaluation

As described in Section 2.3, we evaluated the microstructure and porosity of the prints from two different facilities to obtain a broader sample of operators and individual machines. Figure 6 shows the in-plane metallographic sections through the LBPF as-printed and HIP ring samples from Facility A. Small amounts of scattered microporosity are seen throughout the sample but are more prominent in the thicker sections at the top of the build. Porosity size of up to approximately 0.1 mm (0.004 inch) is apparent. In contrast, following HIP only minute and infrequent remnants of porosity are apparent. Porosity remaining near the printed surface on the HIP samples from Figure 6 (right) appears to be surface connected and therefore would not be removed by HIP. Clearly, HIP eliminated most or all of the significant as-printed porosity.

Facility B produced the results shown in Figure 7. Again, we see small scattered microporosity in the as-printed condition, however

it appears more pronounced in comparison to Facility A. Nearly all pores in the sample from Facility B also appear to have been healed by HIP.

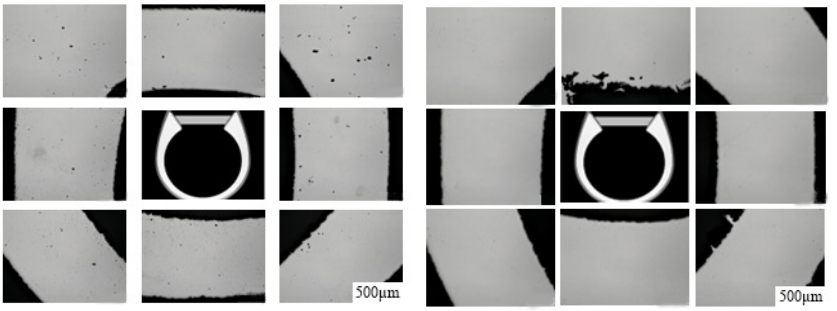

Figure 6: Facility A 950 PtRu LPBF sample in as-printed condition (left) and the HIP condition (right)

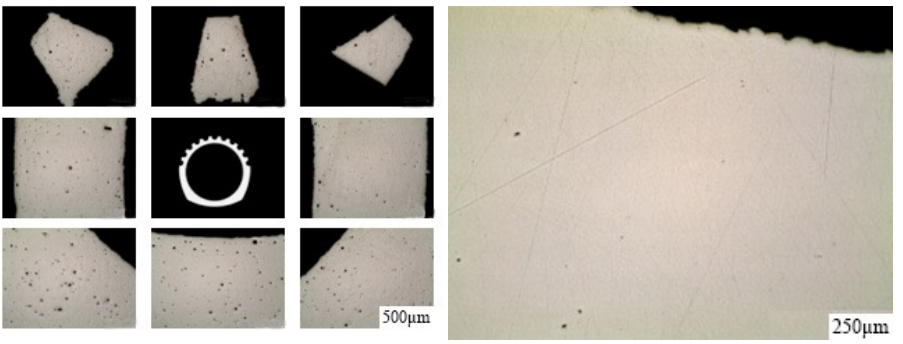

Figure 7: Facility B 950 PtRu LPBF sample in as-printed condition (left) and the HIP condition (right)

Another factor that is very important to consider for platinum alloys is the quality of metallographic sample preparation that determines reported porosity levels when using image analysis.[9] Despite best efforts on the part of the technician, many opportunities exist for incomplete characterization of microstructures. Platinum alloys are very ductile, promoting smearing during polishing that can obscure porosity. The process of sectioning can also miss areas that have greater concentrations of porosity, making evaluations of the bulk material both challenging and costly. To mitigate the risk of such variance our sample preparation was performed by a single lab and operator according to the fixed process sample preparation described in

Section 2.7. Density was characterized using the metallographic sections by image analysis using Pax-it software and porosity values were found to range from roughly 1% to 5%. Ultimately, we elected to not provide precise porosity measurements due to the high number of variables that can affect density interpretation. Visual comparisons are instead relied upon to demonstrate differences between samples in this work.

While the cause of the porosity from both facilities' samples is not fully understood through our efforts, potential causes have been covered through previous research in quite some detail.[1,4,5,6] Figure 8 demonstrates that porosity tends to be associated with unmelted particles in the LBPF sample produced by Facility A. These observations suggest that porosity is due to lack of melting during the LPBF process. Decreased porosity levels have been reported for platinum alloys through increasing heat input by Klotz and Koenig.[5] In addition, this same study noted that porosity levels increased with decreasing hatch distance and increasing laser speed, suggesting to us that parameters for the LPBF samples we tested were likely not optimized given high observed levels of porosity, particularly for Facility B.

It further appears that the reported 22 µm diameter laser spot size used in the LPBF system from Facilities A & B may not entirely melt the larger particles, therefore it is possible that adhered, but not completely fused particles would tend to create crevices between layers that may not fill during subsequent passes. In this case, finer powder or greater heat input would likely decrease the amount of porosity, again underscoring the need for very tightly defined and controlled process parameters in LPBF production.

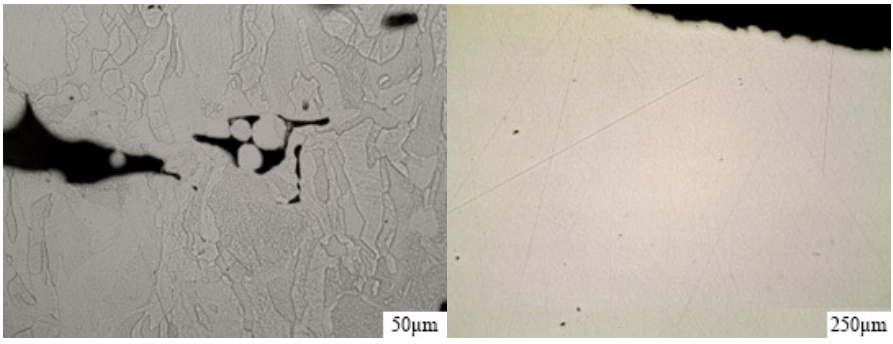

Figure 8: As-polished, in plane metallographic section through the Facility A as-printed LPBF sample

For comparison purposes, Figure 9 demonstrates the same cross-sections from investment cast 950 PtRu. The as-cast section (left) displays abundant, fine, and widely scattered microporosity that is preferentially located toward central locations and consistent with shrinkage porosity. The presence of small spherical voids comingled with asymmetrical shrinkage porosity suggests the presence of gas porosity. Figure 8 (right) demonstrates that like the LPBF product, microporosity is essentially eliminated in the cast product by the HIP process.

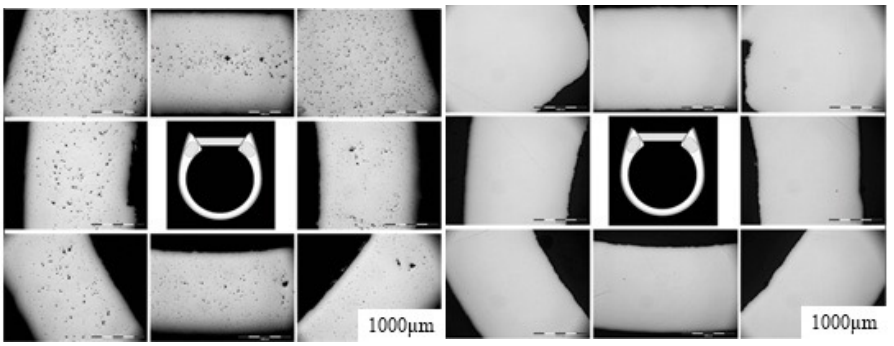

Figure 9: Investment cast 950 PtRu in the as-cast condition (left) and HIP condition (right)

Microstructures revealed by the etched metallographic sections through the as-printed rings appear in Figures 10 and 11. Elongated grains oriented parallel to the build direction suggest epitaxial growth among successive build passes in the Facility A and B samples. Elongated grains in excess of 500 µm far exceed the dimensions of the original powder. The large grain size relative to powder dimensions again suggests epitaxial growth.

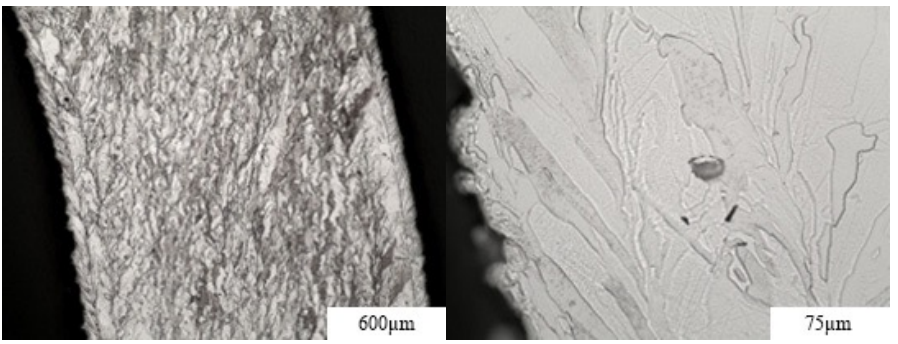

Figure 10: Etched, in-plane metallographic sections through LPBF samples Facility A Ring

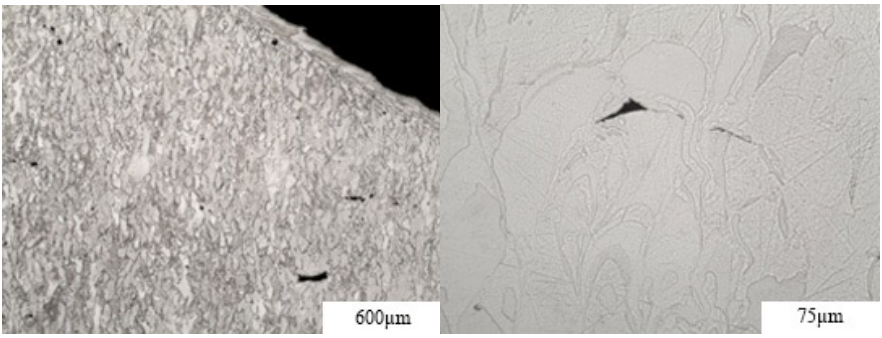

Figure 11: Etched, in-plane metallographic sections through LPBF samples Facility B Ring

Figure 12 displays etched longitudinal metallographic sections through the spent tensile bar gage section of Facility A LPBF as-printed and HIP samples. In all cases, the build direction is out of the plane of the section as shown and the laser travel direction is horizontal. Grains away from the fracture are irregularly shaped and neither equiaxed nor highly elongated. Slight grain elongation in the longitudinal (scan) direction is apparent but not pronounced. An abrupt interface exists between core material and a slightly finer grained near surface layer. The finer grained surface layer is a function of the machine program intended to vary near surface parameters to improve surface finish. Grain growth in the core or near surface material due to the HIP process is not apparent in these samples but has been reported by others for 950 Pt alloys.[1,8] Grain growth as a function of time and temperature suggests that HIP parameters must be adjusted to balance effective porosity elimination with prevention of grain growth, although specific alloys may be more vulnerable in terms of optimizing parameters than others.

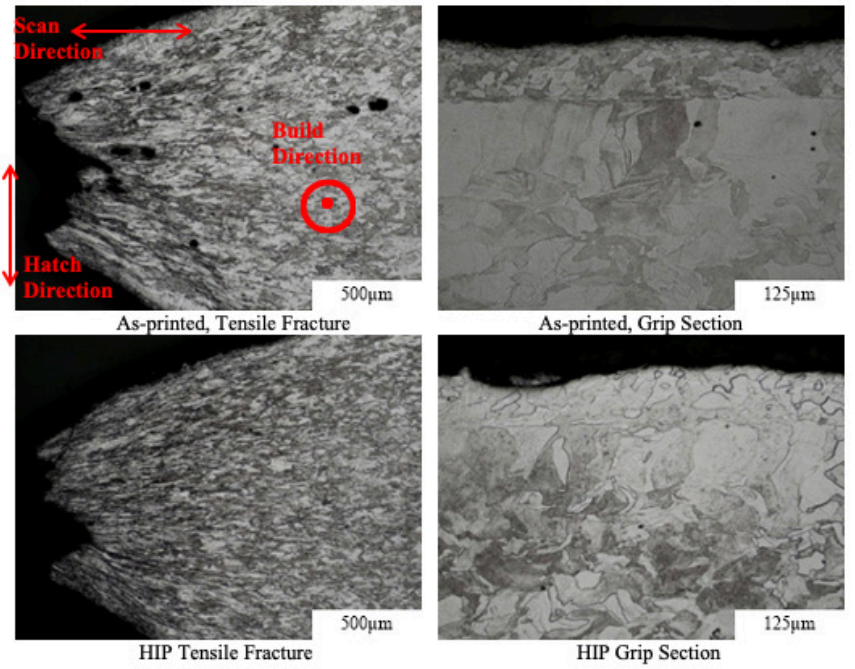

Figure 12: Optical photomicrographs longitudinal sections of spent LPBF as-printed and HIP tensile bars, Facility A.

Etched transverse metallographic sections through the spent tensile bar gage section of as-printed and HIP samples appear in Figures 13 and 14. The location shown is well away from necking and fracture. Grain elongation suggests epitaxial growth between adjacent layers. Angular voids and fine interfaces at porosity appear characteristic of lack of fusion. An absence of spherical shapes suggest that porosity is not due to gas evolution. Significant grain growth due to HIP is not apparent.

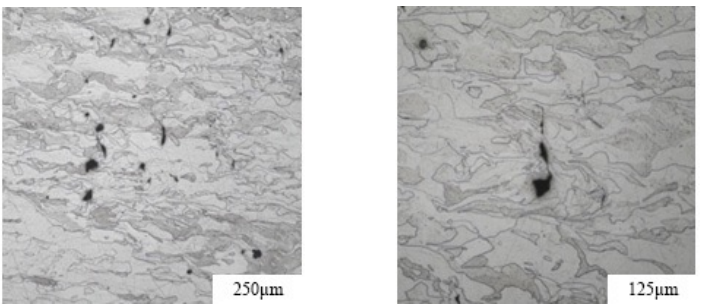

Figure 13: Facility A, As-Printed Tensile Bar, Transverse to Axis

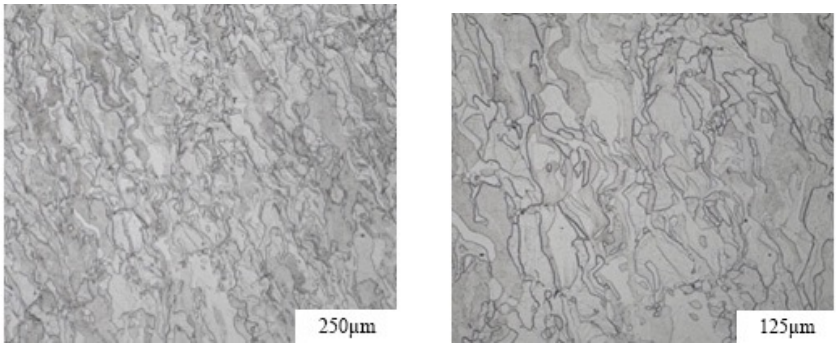

Figure 14: Facility A, HIP LPBF Tensile Bar, Transverse to Axis

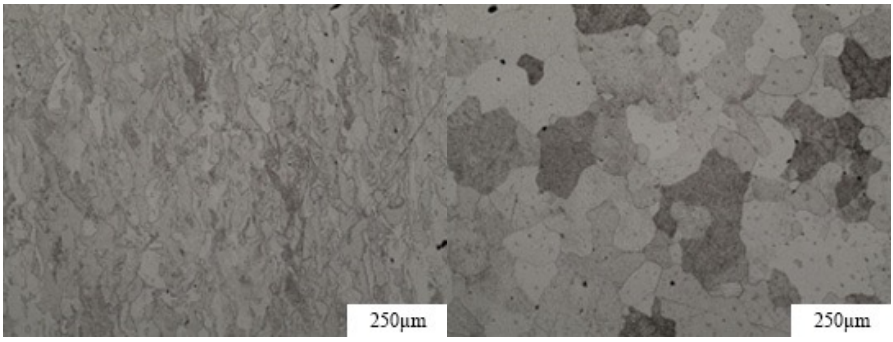

Figure 15: Comparison of LPBF Facility A (left) and investment casting Facility A (right) microstructures

A comparison of LPBF as-printed and investment cast as-cast microstructures appears in Figure 15. The cast microstructure consists of moderately coarse, equiaxed grains, while the printed sample exhibits highly elongated and finer grains. Similar results were obtained from HIP samples. The substantial difference in mechanical properties is consistent with the substantial difference in microstructures. The directional microstructure of the printed bar is consistent with the observed evidence of anisotropy in the spent LPBF tensile bars.

2.4 Surface Finish Characterization

Optical profilometry results acquired from a scan of the top surface of the as-printed LPBF ring sample from Facility A are shown in

Figure 16. The Ra values are the average of 5 linear scans in radial and circumferential directions.

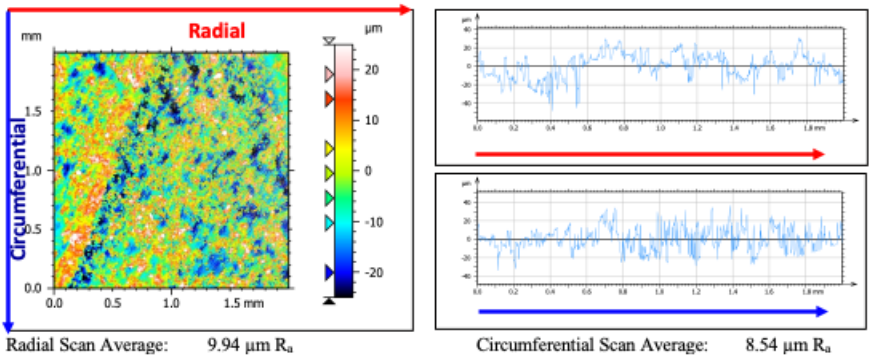

Figure 16: Optical profilometry of as-printed LPBF ring Facility A

Scanning electron microscopy (SEM) of the top surface of the as-printed LPBF ring shown in Figure 17 reveals the clear concentric pattern of the individual laser melts employed by the technology. This topographical condition is one of the contributors to the rougher surface finishes observed in LPBF product. Despite 10 nm vertical resolution, the ripple pattern of the deposits is not revealed by optical profilometry.

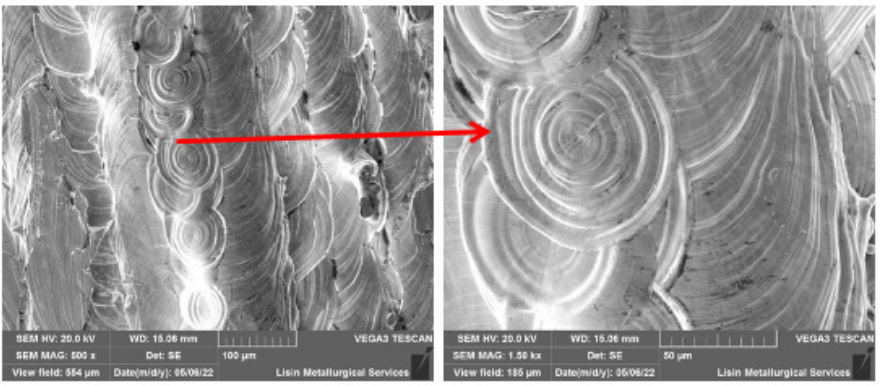

Figure 17: SEM image of as-printed 950 PtRu LPBF Facility A

Optical profilometry results acquired from a scan of the top surface of the LPBF sample in the HIP condition are shown in Figure 18. The Ra values are the average of 5 linear scans in radial

and circumferential directions. The HIP samples slow a slight improvement in the Ra values, suggesting surface tension driven diffusion during the HIP process.

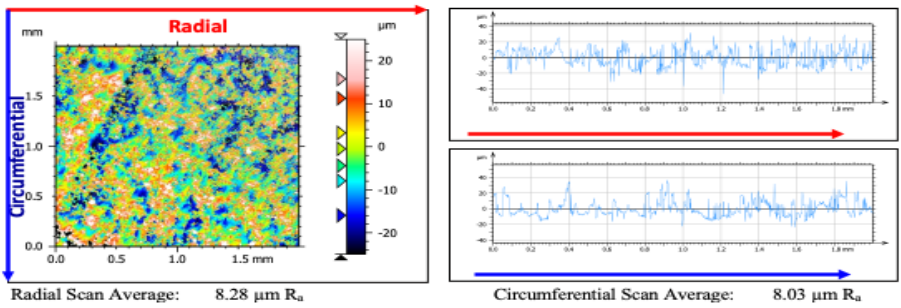

Figure 18: Optical Profilometry of LPBF HIP Sample Facility A

SEM of the surface of the HIP LPBF sample shown in Figure 19 reveals a blending of the concentric features that were present in the as-printed condition. The small spheres are likely loose particles of powder that were sinter-bonded during the LPBF printing and further bonded during the HIP process.

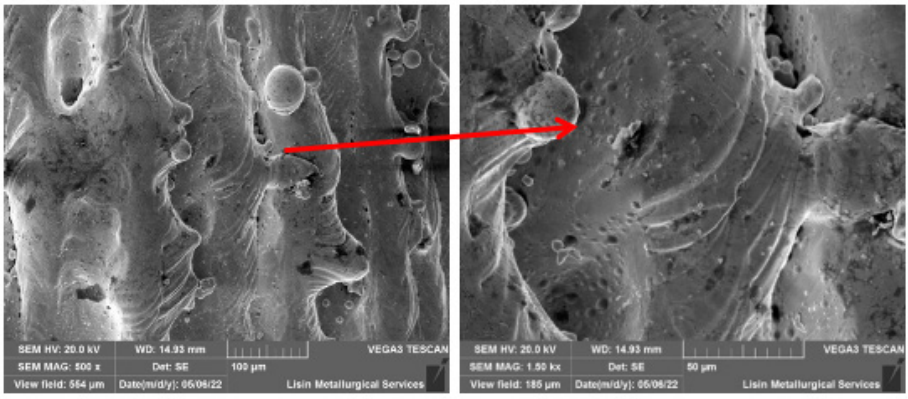

Figure 19: SEM image of 950 PtRu LPBF sample in the HIP condition Facility A

For comparison, we measured 950 PtRu investment casting roughness using a 3D confocal profilometry scan of a representative surface of a cast ring (Figure 20). Perpendicularly oriented roughness profiles were extracted from this scan and

averaged to be 0.9 µm Ra. The cast sample is notably smoother than the LPBF samples.

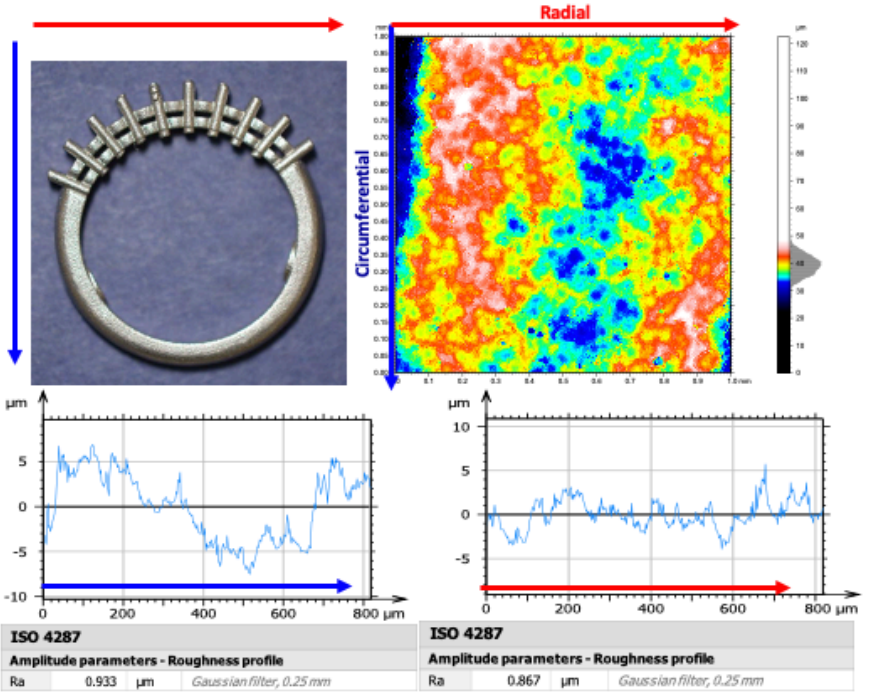

Figure 20: Surface roughness of cast 950 PtRu: 0.9 µm Ra average

CONCLUSIONS

1. Mechanical properties and specifically strength and hardness of LPBF 950 PtRu were found to be superior to mechanical properties of the same alloy produced through investment casting. A 93% increase in yield strength (YS) MPa value and a 30% increase in ultimate tensile strength (UTS) MPa value was observed in the as-printed LPBF samples compared to as-cast test bars, and for HIP samples an increase of 49% and 19% respectively was observed. It is notable that the tensile properties for the as-printed LPBF test bars maintained high levels of strength and ductility in comparison to cast product despite the presence of porosity.
2. Hardness also shows an increase for the LPBF samples in the range of 25% for as-printed, as-cast, and HIP conditions.
3. Of note is the significant drop in YS and UTS in the HIP condition for the LPBF samples which may be attributed to annealing of the highly stressed, high dislocation density as-

deposited structure.

4. Grain size was found to be substantially smaller in the 950 PtRu LPBF alloy relative to the cast alloy, and the above-referenced increase in strength and hardness properties is at least in part due to this finer grain size.
5. The ductility properties of elongation and reduction of area for 950 PtRu LPBF samples were very close to that of cast alloy; this holds true for the as-printed, as-cast, and HIP conditions.
6. Substantial porosity was apparent in 950 Pt LPBF 950 Pt samples produced at both facilities. Although the cause of the porosity was not fully explored in this work, our observations suggest it is associated with a lack of fusion. Previous research has attributed higher levels of porosity and lack of fusion to non-optimal heat, hatch distance, laser speeds, and powder fineness.
7. Porosity is effectively removed by HIP in both LPBF and cast 950 PtRu although trade-offs exist in terms of lower YS and UTS in LPBF samples. HIP is not readily available to all manufacturers; therefore optimization, control, and consistency of LPBF as-printed density is a very desirable goal.
8. HIP of metals is widely employed in the AM industry and this work and other work has demonstrated the effectiveness of the technique with respect to porosity removal.[1] Despite the false sense of precision created by precise image analysis measurements of percent porosity, we conclude that minor porosity is 1) common in LPBF manufactured platinum alloys, 2) readily removed by HIP, and 3) challenging to accurately and reliably characterize on soft, ductile Pt alloys by standard metallographic techniques.
9. Average surface roughness of as-printed LPBF components from Facility A (9.24 Ra average) is inferior to that of cast components (0.9 Ra). However, these trials did not pursue the benefits of surface finish optimization through modified parameters or mass finishing techniques that have demonstrated to improve surface finishes on LPBF products.[3]
10. Variables such as build layer height, scan speed, energy inputs, hatch spacing and powder quality can all impact density levels.[1,5] Given the broad range of reported density levels for LPBF outputs and characterization of surface finishes, the data suggests there may be a trade-off between build parameters that optimize one over the other. Further studies exploring this topic would be beneficial to the industry.

REFERENCES

1. Laag, T. and Heinrich, J., "Powder Processing of Platinum Group Metals: Advantages and Challenges", *Santa Fe Symposium 2018*, Met-Chem Research, ABQ, NM, USA, 2018: pp. 327–343.
2. Frye, T. and Fischer-Buehner, J., "Platinum Alloys in the 21st Century: A Comparative Study", *Santa Fe Symposium 2011*, Met Chem Research, ABQ, NM, USA 2011: pp 201-229
3. Zito, D., "Definition and Solidity of Gold and Platinum Jewelry Produced Using Selective Laser Melting (SLM) Technology" *Santa Fe Symposium 2015*, Met Chem Research, ABQ, NM, USA 2015: pp 455-492
4. Zito, D., "Potential and Innovation of Selective Laser Melting Technique in Platinum Jewelry Production" *Santa Fe Symposium 2018*, Met Chem Research, ABQ, NM, USA 2018: pp 625-684
5. Klotz, U. and Koenig, F., "Additive Manufacturing of Platinum Alloys: Practical Aspects during LPBF of Jewellery Items", Jewelry Technology Forum 2022, Vicenza, Italy, https://www.youtube.com/watch?v=VK9USeEhVH0
6. Strauss, J., "Additive Manufacturing of Precious Metals", ASM Handbook 2020 Vol 24, pp.
7. Frye, T. and Klotz, U., "Mechanical Properties and Wear Resistance of Platinum Jewelry Casting Alloys: A Comparative Study" *Santa Fe Symposium 2017*, Met Chem Research, ABQ, NM, USA 2017: pp 1-40
8. Frye, T. and Klotz, U., "The Effects of Hot Isostatic Pressing of Platinum Alloy Castings on Mechanical Properties and Microstructures" *Santa Fe Symposium 2014*, Met Chem Research, ABQ, NM, USA 2014: pp 1-22
9. P. Battaini, "Metallography of Platinum and Platinum Alloys" *Santa Fe Symposium 2010*, Met Chem Research, ABQ, NM, USA 2010: pp 27-49